OAK RIDGE NATIONAL LABORATORY LIBRARIES
3 4456 0549914 5

CENTRAL RESEARCH LIBRARY
DOCUMENT COLLECTION

OAK RIDGE NATIONAL LABORATORY
operated by
UNION CARBIDE CORPORATION
NUCLEAR DIVISION
for the
U.S. ATOMIC ENERGY COMMISSION

ORNL-TM-1444

2

AN APPARATUS FOR MEASUREMENT OF ELECTRON ATTACHMENT AND ELECTRON SWARM DRIFT VELOCITIES AT HIGH TEMPERATURES

(Thesis)

W. G. Hendrick, L. G. Christophorou, and G. S. Hurst

OAK RIDGE NATIONAL LABORATORY
CENTRAL RESEARCH LIBRARY
DOCUMENT COLLECTION
LIBRARY LOAN COPY
DO NOT TRANSFER TO ANOTHER PERSON
If you wish someone else to see this document, send in name with document and the library will arrange a loan.

Submitted by W. G. Hendrick as a thesis to the Graduate School of the University of Tennessee in partial fulfillment of the requirements for the degree of Master of Science.

LEGAL NOTICE

This report was prepared as an account of Government sponsored work. Neither the United States, nor the Commission, nor any person acting on behalf of the Commission:

A. Makes any warranty or representation, expressed or implied, with respect to the accuracy, completeness, or usefulness of the information contained in this report, or that the use of any information, apparatus, method, or process disclosed in this report may not infringe privately owned rights; or

B. Assumes any liabilities with respect to the use of, or for damages resulting from the use of any information, apparatus, method, or process disclosed in this report.

As used in the above, "person acting on behalf of the Commission" includes any employee or contractor of the Commission, or employee of such contractor, to the extent that such employee or contractor of the Commission, or employee of such contractor prepares, disseminates, or provides access to, any information pursuant to his employment or contract with the Commission, or his employment with such contractor.

ORNL-TM-1444

Contract No. W-7405-eng-26

HEALTH PHYSICS DIVISION

AN APPARATUS FOR MEASUREMENT OF ELECTRON ATTACHMENT AND ELECTRON SWARM DRIFT VELOCITIES AT HIGH TEMPERATURES

W. G. Hendrick, L. G. Christophorou, and G. S. Hurst

Submitted by W. G. Hendrick as a thesis to the
Graduate School of the University of Tennessee
in partial fulfillment of the requirements
for the degree of Master of Science

FEBRUARY 1968

OAK RIDGE NATIONAL LABORATORY
Oak Ridge, Tennessee
operated by
UNION CARBIDE CORPORATION
for the
U. S. ATOMIC ENERGY COMMISSION

OAK RIDGE NATIONAL LABORATORY LIBRARIES

3 4456 0549914 5

ACKNOWLEDGEMENTS

The authors wish to acknowledge the assistant of J. A. Harter, D. Pittman, and J. T. Cox.

TABLE OF CONTENTS

CHAPTER		PAGE
I.	GENERAL INTRODUCTION	1
II.	EXPERIMENTAL EQUIPMENT	11
	Chambers	11
	Vacuum, Gases, Purification	18
	Electronics and Data Readout	22
	Heating System	28
III.	FUNCTIONING OF THE APPARATUS AND EXPERIMENTAL PROCEDURE	36
IV.	RESULTS AND DISCUSSION	41
	Electron Attachment to SF_6	41
	Temperature Dependence of the Attachment Rates in SF_6	43
	Electron Drift Velocities in Nitrogen and Ethylene as a Function of Temperature	47
	Drift velocities in nitrogen	47
	Drift velocities in ethylene	52
	Velocity Dependence and Magnitude of the Cross Section for Momentum Transfer in Ethylene	52
V.	CONCLUSIONS	57
BIBLIOGRAPHY		58

LIST OF TABLES

TABLE		PAGE
I.	Attachment Cross Sections for SF_6^-	46
II.	Electron Swarm Drift Velocities in Nitrogen at Various Temperatures	48
III.	Electron Swarm Drift Velocities in Ethylene at Various Temperatures	49
IV.	Temperature Dependence of w(T) for Various Values of α	54

LIST OF FIGURES

FIGURE		PAGE
1.	Schematic of Electron Attachment in a Uniform Electric Field	5
2.	Calculated Dependence of Pulse Height on τ_o/t_1 for Various Values of f	7
3.	Ionization Chamber for Measurement of Attachment Coefficients and Electron Drift Velocities at High Temperatures	12
4.	High Temperature Electron Attachment Apparatus	13
5.	Photograph of Equipment	14
6.	Circuit of Preamplifier Used in Electron Attachment Studies	24
7.	a) Ultraviolet Xenon Light Source Schematic; b) Photodiode Schematic	25
8.	Diagram of Heating System	32
9.	Diagram of Heater Wiring	34
10.	Measured Response of the Linear Amplifier	37
11.	Temperature Dependence of the Electron Attachment Rates in SF_6	44

FIGURE PAGE

12. Electron Drift Velocities in Nitrogen versus E/P for 298° and 473° K. 50

13. Electron Drift Velocities in Ethylene versus E/P for 298° and 473° K. 51

14. Experimental and Calculated Values of w (for $\alpha = 0$) as a Function of Temperature for Various E/P 56

CHAPTER I

GENERAL INTRODUCTION

Free electrons of low energies (< 10 eV.) interact readily with complex molecules. [See, for example, Christophorou and Compton (1967).] Free electrons at these very low energies can be produced as an electron swarm of known electron energy distribution or as a monoenergetic electron beam.

The nature of the electron-molecule interaction is not yet fully understood in spite of its importance in the fields of radiation physics, radiation chemistry, and radiation biology. Although the behavior of free electrons in a gas may be different from that in a biological system, knowledge of the electronic properties of biologically important molecules in the gas phase is fundamental and basic.

In electron attachment studies it is extremely important to distinguish between the various ways by which an electron can be attached to a molecule. Three such ways can be distinguished in the gas phase.

1. Temporary nondissociative electron attachment,

$$AX + e \rightleftarrows AX^{-*} \tag{1}$$

The lifetime of the temporary negative ion is determined by internal rearrangement and by molecular collision. If an equilibrium is reached, the ion density, n_i/n_e, is

determined by the molecular electron affinity, E_o, i.e.,

$$n_i/n_e = \text{const}\ e^{E_o/kT} \quad . \tag{2}$$

2. Permanent nondissociative electron attachment,

$$AX + e \rightarrow AX^{-*} \rightarrow AX^- + \text{energy}\,. \tag{3}$$

The excited negative ion, AX^{-*}, has to be stabilized by radiation or by collision.

3. Dissociative electron attachment,

$$AX + e \rightarrow A(A^*) + X^- \,. \tag{4}$$

No collisional stabilization is required for this process.

Frequently, the electron attachment processes are studied by two experimental methods: the electron swarm and the electron beam. In the electron swarm method electrons are set free in a gas by various means, such as ionization by energetic charged particles, ultraviolet radiation, or thermionic emission. These free electrons make many collisions with the atoms or the molecules of the gas through which they pass in the presence of an electric field, and they have a wide distribution in their kinetic energies. Regardless of their energy of liberation they come into an equilibrium energy distribution which is characteristic of the gas through which they travel and the ratio E/P, the pressure reduced electric field in volts cm.$^{-1}$ torr^{-1}. This equilibrium energy distribution results

from energy losses by collisions with atoms or molecules and energy gained from the electric field. The drift velocity, w, of the electron swarm is much less than the average agitation speed of the random motion of the electrons [Huxley and Crompton (1962)]. The distribution of electron energies in an electron swarm is characterized by a function $f(\epsilon, E/P)$ which depends on the gaseous medium and E/P. Generally, certain non-electron-attaching carrier gases (e.g., C_2H_4, N_2, Ar) are used to determine the electron energy distribution, $f(\epsilon, E/P)$ [Stockdale and Hurst (1964), Christophorou et al. (1965)].

The function $f(\epsilon, E/P)$ is defined as $f(\epsilon, E/P)d\epsilon \equiv$ fraction of electrons in an energy range $d\epsilon$ about ϵ, where ϵ is the electron energy. Electron swarm experiments measure quantities which are averaged over $f(\epsilon, E/P)$. Furthermore, swarm experiments do not, generally, lead to identification of the particular kinds of processes involved; e.g., in electron attachment studies by the swarm technique the various types of ions formed are not distinguishable.

In beam experiments, on the other hand, the electron energy distribution is much more nearly "monochromatic." Thus, data obtained by use of beams may be regarded as giving, to a first approximation, the shape of the attachment cross section as a function of electron energy [see, however, Christophorou et al. (1967)]. Furthermore, when electron beam experiments are incorporated with mass analysis methods, information on the specific

types of ions formed is obtained. One of the main deficiencies in beam experiments is that knowledge of absolute cross sections for electron attachment is very difficult to obtain.

Among the various electron swarm methods used for the measurement of electron attachment to molecular gases is that of Bortner and Hurst (1958). The effect of electron attachment on the pulse height in a plane parallel ionization chamber was chosen as the physical basis of measuring the attachment coefficient in the method of Bortner and Hurst. Briefly, the physical basis of the method is as follows. If N_o electrons are formed at a distance d from a positive collector, then at a distance x from the point of formation only N electrons will be unattached, the rest being attached (see Figure 1). The number of electrons dN attached in dx is

$$dN = -\alpha f_1 P \, dx \tag{5}$$

where α is the attachment coefficient and $f_1 P$ is the partial pressure of the attaching gas.

The time variation of the positive electrode potential is

$$V(t) = \frac{A}{f}\left(1 - e^{-f(t/\tau_o)}\right) \tag{6}$$

where $A = N_o V_o$, $f = \alpha f_1 Pd$, τ_o = collection time, and V_o = the change in the collector potential due to a single electron moving the entire distance d.

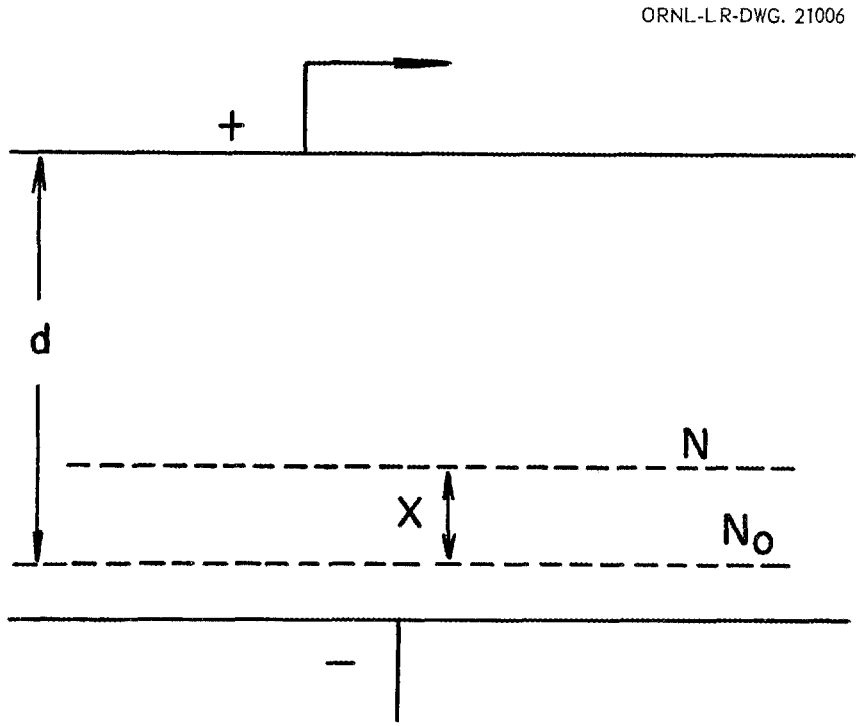

Figure 1. Schematic of electron attachment in a uniform electric field.

If the pulse given by Equation (6) is observed with a linear amplifier having a response to a step function as

$$V'(t) = \frac{t}{t_1} e^{-t/t_1}, \tag{7}$$

where t_1 is both the differentiating and integrating time constants (here assumed equal), the output of the pulse amplifier will then be given by

$$V(\tau) = \int_0^{\tau_0} \frac{dV(t)}{dt} V'(\tau - t)\, dt \tag{8}$$

for $\tau > \tau_0$.

Integrating Equation (8), we get the pulse height $V(\tau)$ which has a maximum value, $V(\tau')$, at $\tau = \tau' \geq \tau_0$. The pulse height is plotted in Figure 2 as a function of τ_0/t_1 for various values of f. These curves may then be used to calculate the attachment coefficient (the probability of capture per cm. traveled in the field direction per torr of attaching gas) from the experimentally measured quantities $V(\tau')$ and τ_0.

In the original method electrons are produced by α-particle ionization (from a Pu^{239} source) in a plane normal to the applied electric field at a fixed distance from a collecting electrode (see Chapter II). The pulse height and the collection time are measured both for the carrier gas and the mixture containing the carrier gas and the attaching gas. The attaching gas is added to the carrier gas at a pressure f_1P which is less

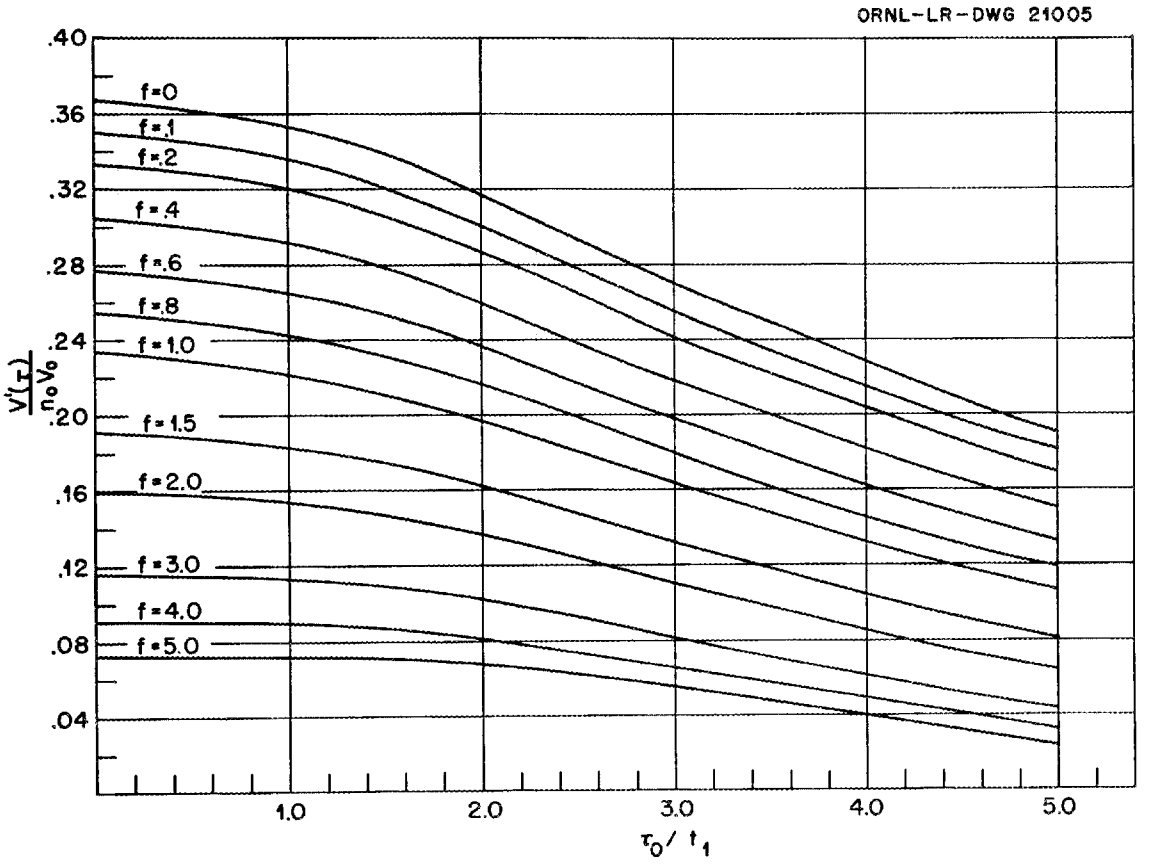

Figure 2. Calculated dependence of pulse height on τ_0/t_1 for various values of f.

than the pressure of the carrier gas, f_2P, such that $f(\epsilon, E/P)$ is characteristic of the carrier gas alone. By choice of the carrier gas and E/P, $f(\epsilon, E/P)$ can be set to peak over the energy range from thermal to ~ 10 eV. [Stockdale and Hurst (1964), Christophorou et al. (1965)].

Swarm experiments measure the quantity $\alpha(E/P) \times w(E/P)$ which is the absolute rate at which electrons are removed from the electron swarm due to attachment. This quantity is related to the attachment cross section, $\sigma_c(\epsilon)$, and the electron energy, ϵ, by

$$\alpha(E/P) \times w(E/P) = N(2/m)^{\frac{1}{2}} \int_0^\infty \epsilon^{\frac{1}{2}} \sigma_c(\epsilon)\, f(\epsilon, E/P) d\epsilon \tag{9}$$

where N is the number of attaching gas molecules per cm.^{3} at 1 torr and m is the electron mass.

Recently, Christophorou et al. (1965) described a swarm-beam technique in which they combine electron swarm and electron beam data to obtain absolute attachment cross sections as a function of electron energy and also to achieve an independent energy calibration for as low as a few tenths of an eV. In this technique the difference ion current as a function of electron energy, $I(\epsilon)$, (obtained from beam experiments) is assumed to be related with $\sigma_c(\epsilon)$ through the following relationship:

$$\sigma_{cj}(\epsilon) = K_j T_j I(\epsilon) \tag{10}$$

where T_j is an operator which translates $I(\epsilon)$ along the energy axis and K_j is the constant of proportionality between $\sigma_{cj}(\epsilon)$ and $I(\epsilon)$. Relation (10) combined with Equation (9) allows determination of both T_j and K_j when $\alpha(E/P) \times w(E/P)$ and $I(\epsilon)$ are known. This has been done by obtaining through a least squares procedure the best fit to the experimental data, i.e.,

$$\frac{d}{dT_j}\left\{ \sum_i \left[N(2/m)^{\frac{1}{2}} K_j \int_0^\infty \epsilon^{\frac{1}{2}} T_j I(\epsilon) f_i(\epsilon) d\epsilon - \alpha_i w_i \right]^2 \right\} = 0 \qquad (11)$$

where the subscript i specifies a given value of E/P; $\alpha_i w_i$ are the experimental swarm attachment rates, and the other term in Equation (11) is the calculated attachment rate. The optimum translation, $T_j(\text{opt})$, and the corresponding value for K_j can be calculated from Equation (11) and upon substitution into Equation (10) $\sigma_c(\epsilon)$ can be obtained. In principle any trial function can be tested; however, Christophorou et al. (1965) used expression (10) since it led to rapid and satisfactory solution of Equation (11). Application of this method has been made to the study of electron attachment processes for a number of molecules [Compton and Christophorou (1967), Christophorou et al. (1967)].

The present study is part of a general effort to understand the physics of electron-molecule interactions. Specifically in this report we describe an apparatus which can be used to study $\alpha(E/P)$, $w(E/P)$, and

$\alpha(E/P) \times w(E/P)$ as a function of temperature. Since the first development of the Bortner and Hurst (1958) technique, the method has remained basically unchanged although various modifications were made to the old system. A new design of the parallel plate ionization chamber, for example, has been described by Christophorou et al. (1965). The new experiment, which we describe here, is based on the same physical principles as the old arrangement but is improved in a number of ways and is modified to permit electron attachment studies at temperatures from 295° to 500° K.

The details of the method will be described in Chapter II and the functioning of the apparatus as well as the experimental procedure will be discussed in Chapter III. In Chapter IV data will be presented on the temperature dependence of the thermal electron attachment rates in SF_6 and the temperature dependence of the thermal electron-swarm drift velocities in the carrier gases N_2 and C_2H_4 ($298° \leq T \leq 473°$ K.).

CHAPTER II

EXPERIMENTAL EQUIPMENT

The basic equipment consists of the following main parts (see Figures 3, 4, and 5): chambers; vacuum system, purification system, gauges, and gases; electronics and data readout; and heating system.

I. CHAMBERS

The sensitive part of the whole apparatus is a parallel plate ionization chamber (see Figure 3). The chamber assembly is a gold-plated cylinder inside of which are two gold-plated plates, the collector C and, 9 cm. away, the emitter EM. Also, at a distance of 7 cm. from C the Pu^{239} "O-ring-type" α-emitter is located. The plate EM forms the lower end of the drift space and is held at a negative potential, while the collector C is held at a virtual ground and constitutes the upper end of the drift space. Plate EM is the photosurface from which electrons are ejected by ultraviolet radiation when drift velocities are to be measured. A gas discharge tube, G. M., is mounted to the plate C for use in drift velocity measurements. For pulse height measurements the ultraviolet light is off and the electron swarms are produced at a distance of 7 cm. (rather than 9 cm.) by α-particle ionization. The ionization chamber has

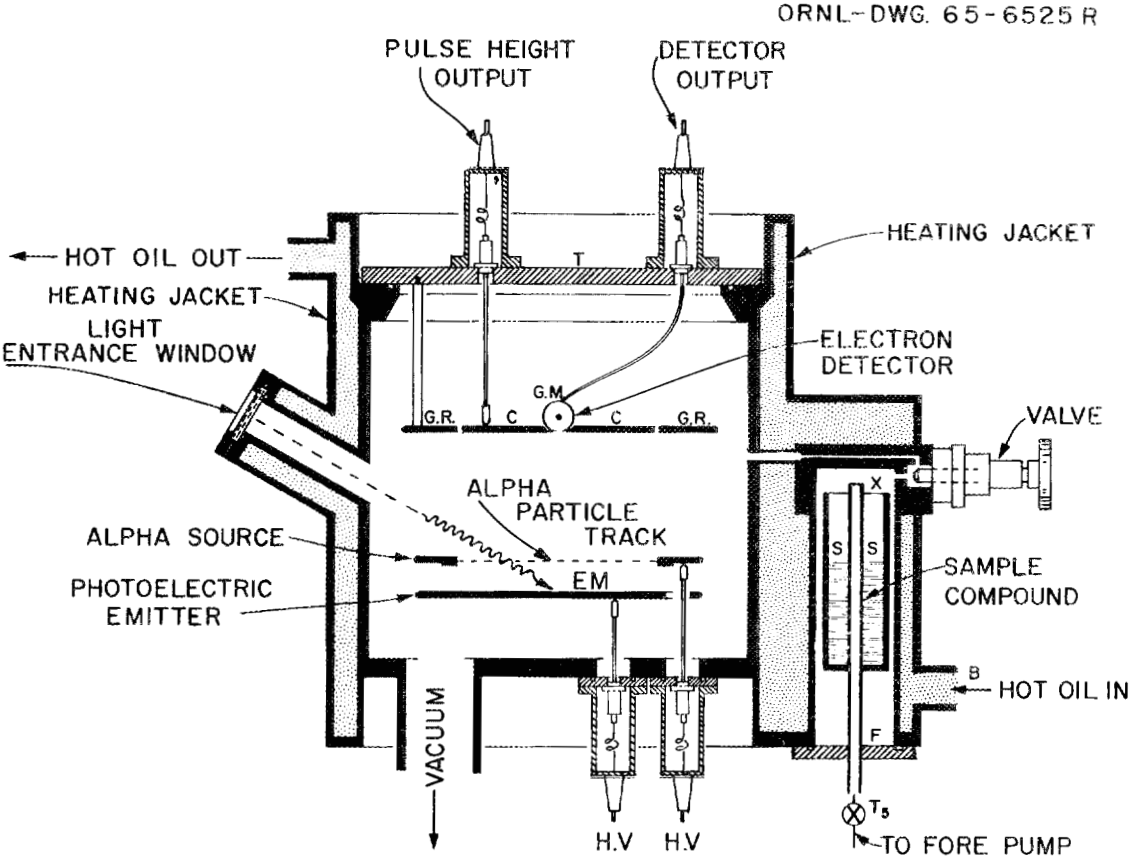

Figure 3. Ionization chamber for measurement of attachment coefficients and electron drift velocities at high temperatures.

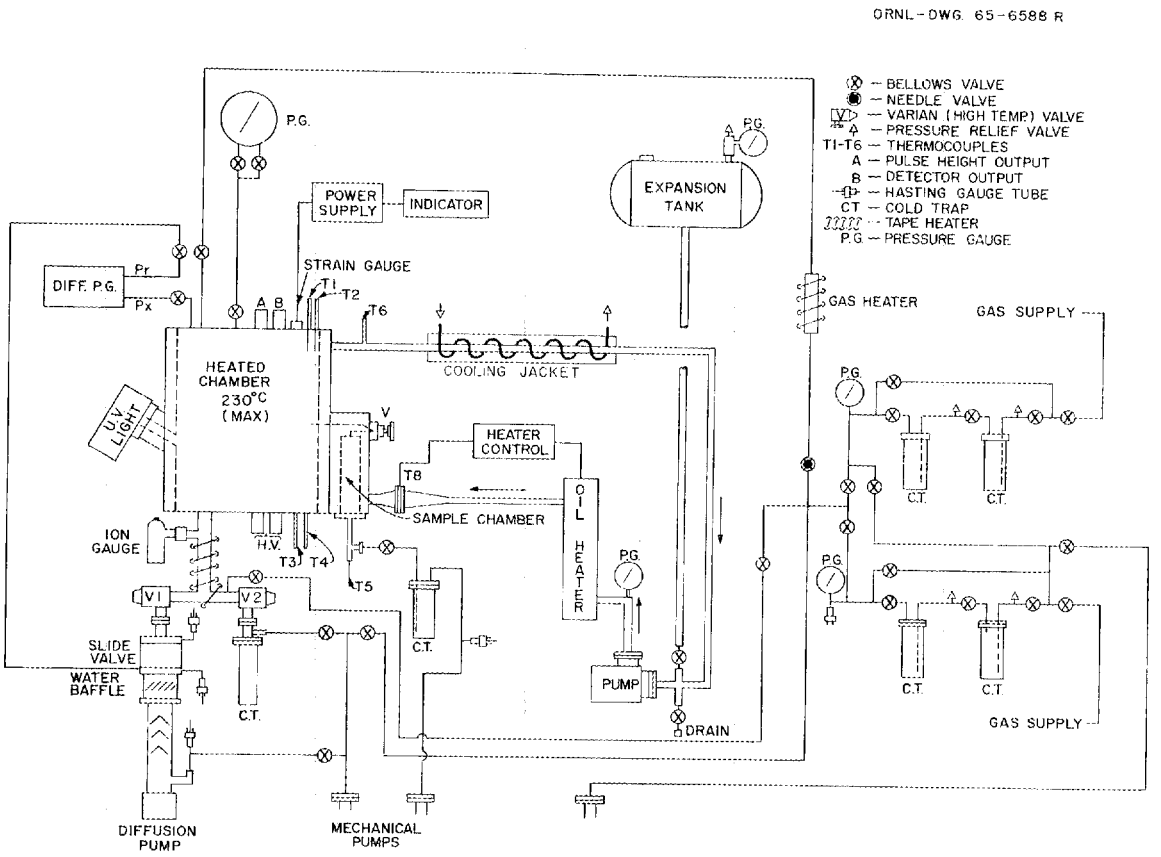

Figure 4. High temperature electron attachment apparatus.

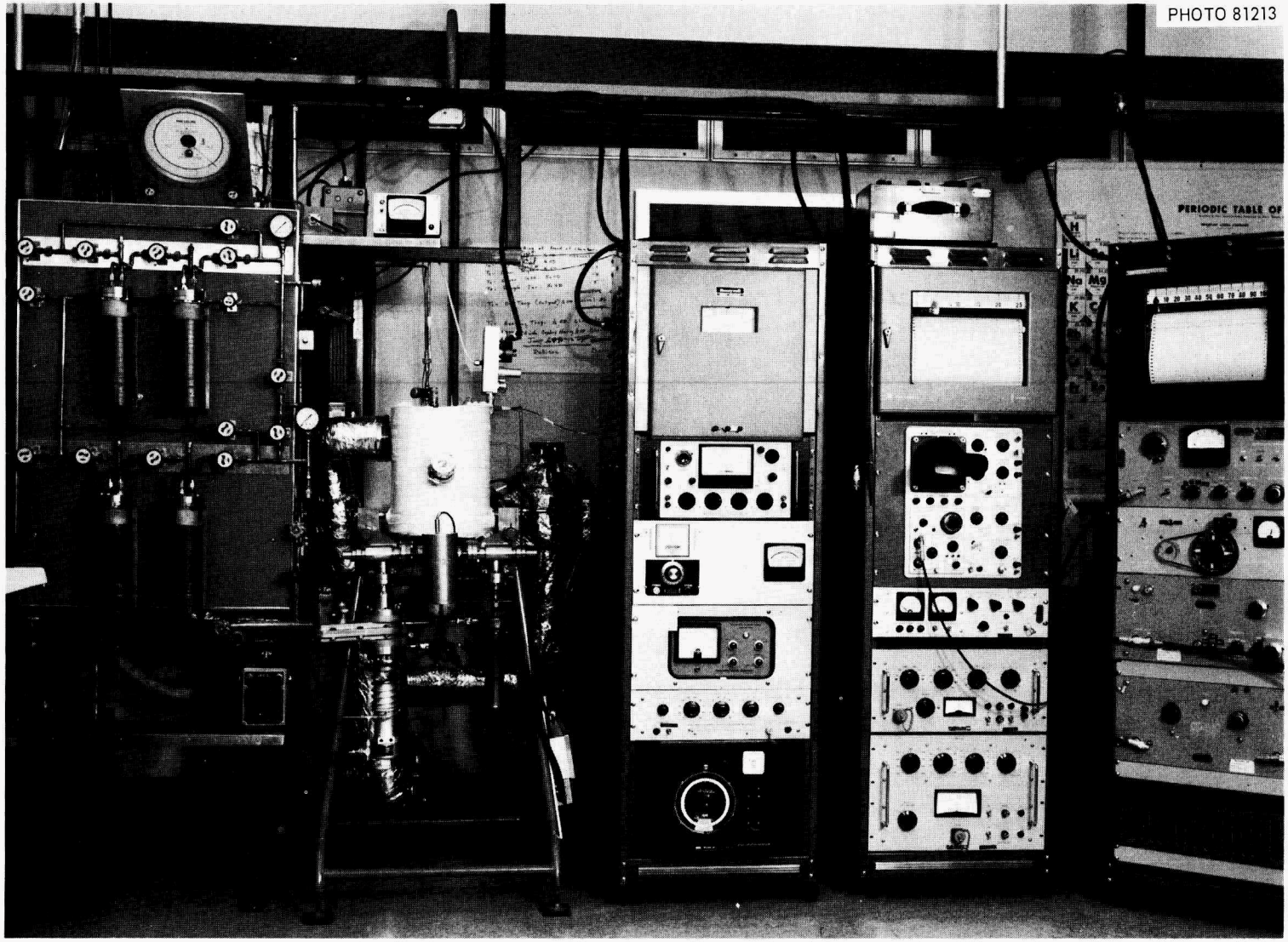

Figure 5. Photograph of equipment.

a quartz window to allow transmission of the ultraviolet radiation. Among the various changes and improvements which were made to the main chamber to allow reduction of outgassing (very important at high temperatures), better vacuum and improved operating conditions are the following:

(i) The chamber was milled out of a solid billet of mild steel (rather than being put together in parts) to eliminate "O-rings." Flanges were eliminated from the top plate T which was made of polished stainless steel baked in a vacuum at 200° C. for 24 hours. A polished finish of less than 8 r.m.s. was necessary in order to get the upper plate to seal on its "O-ring" over the temperature range specified earlier. "O-rings" were removed from the pulse height output, detector output, and high voltage inputs. Instead, a fitting was constructed so that the output leads could be taken through silver-soldered insulators. The high voltage leads were silver-soldered to Ceramaseal alumina insulators, which were installed with Varian flanges. The various plates inside the chamber were gold-plated brass. All screws, insulators, and supports used inside the main chamber were slotted or groved to enable rapid and efficient pump-out of the chamber.

(ii) Another improvement was the suspension of the collector plate C and the associated guard ring G.R. from the top plate T rather than having them located at a fixed position as was done by Hurst and Bortner (1959), Stockdale and Hurst (1964), and Christophorou _et al._ (1965).

(iii) In the previous system plate C was 0.0625 in. thick. In the present arrangement of a heated chamber it was thought necessary to increase the thickness of plate C (to increase dimensional stability), but in doing so the capacitance between C and G.R. was increased. Several attempts were made to reduce this capacitance. The major reduction was achieved by milling and lapping the outer edge of plate C and the inner edge of the guard ring G.R. The 26 μμF. capacitance finally achieved showed a change of approximately 3.5 per cent over the temperature range stated.

(iv) The fluorothene insulators used in the old arrangements have appreciable vapor pressure even at room temperature. At higher temperatures this is highly undesirable since fluorene atoms are good electron acceptors. "Lavite" insulators have been used instead and this was an improvement in terms of outgassing and contamination of the gas mixtures under investigation.

(v) The Pu^{239} α-source was prepared as in the old system [Christophorou _et al._ (1965)]. Pu^{239} was plated and backed on a 0.01 in. thick platinum strip. We counted 26,000 pulses per minute which is a good counting rate for these experiments. One modification, however, was introduced; the upper collimating ring was split into two halves to allow proper positioning of the platinum strip into the circular channel of the lower collimating ring.

(vi) The gas discharge tube was also re-designed. It was found that excess metal near the entrance hole reduced the G. M. tube counting efficiency. A slot, therefore, was milled in the collector plate C which reduced the wall thickness of the G. M. tube such that the thickness of the metal around the hole (0. 0625 in. in diameter) was less than 0. 006 in. The G. M. tube was gold-plated brass (0. 75 in. outside diameter; 0. 035 in. wall thickness; 3. 625 in. length). The present increase in length of the G. M. tube was necessary to increase the pulse output. The anode wire used was made of tungsten and was 0. 003 in. in diameter.

The second chamber, X, contains the stainless steel sample container (Figure 3, page 12). A removable stainless steel cup, S, (Figure 3) was attached to the sample chamber cover plate, F, by a stainless steel tube. The sample, cup S, and thermocouple T_5 were all removable as a unit. Both the main ionization chamber and the sample chamber are always kept at the same temperature. A 0. 5 in. long stainless steel tube connects the chamber, X, with the main chamber through a stainless steel Nuclear Products valve.

A mild steel jacket was constructed around the two chambers for heating. Preheated oil was introduced at two places, A and B. B is on the sample side (see Figure 3), and A is 90° from B and tangent to the main chamber wall. To obtain direction flow an annealed copper helix was soldered to the main chamber. The helix extends to

within 0.0313 in. of the outer wall; it actually forms a rectangular tube (0.5 in. wide and 1.5 in. high) which extends from the oil entrance ports to the oil exit port.

Five stainless steel sheathed, gold-plated thermocouples, T_1 to T_5, (see Figure 4, page 13) were used to indicate the temperature at different points in the two chambers. Thermocouple T_1 was ~ 0.25 in. above G.R., while T_2 was closer to the top plate T and near the carrier gas input line to indicate any changes in temperature when the carrier gas was introduced. Thermocouples T_3 and T_4 enter from the bottom of the main chamber. T_3 was located near the emitter plate EM to indicate any possible temperature changes near the bottom of the plate. T_4 extends halfway into the drift space but close enough to the chamber walls not to interfere with the field. Experience has shown that this thermocouple was not efficiently heated by radiation from the walls, i.e., T_4 read the same temperature as T_1, T_2, and T_3 only if there was a conducting gas in the chamber. Thermocouple T_5 showed the temperature of the sample (for details on thermocouples, see Section IV of this chapter).

II. VACUUM, GASES, PURIFICATION

One mechanical pump was used for evacuation of the main chamber and the gas system. A second pump was used to evacuate the sample chamber. The vacuum reached by the mechanical pumps alone was of the

order of 30 microns. A vacuum diffusion pump, type MCF 300 (Consolidated Vacuum Corporation), connected with a vacuum pump was used to evacuate the main chamber. A water-cooled baffle, type BW-40 (Consolidated Vacuum Corporation), was used above the diffusion pump to prevent back diffusion of pump oil. The vacuum achieved was measured by an ionization gauge, type G-IC-110A (Consolidated Vacuum Corporation), and was of the order of 10^{-7} torr which is satisfactory for these experiments. When the chamber was isolated from the pumping system, the outgassing rate was 0.1×10^{-3} torr per hour. The bottom of the main chamber connects to a "T" manifold which is terminated in two stainless steel high pressure Varian valves, type 2077 (Varian Associates). This manifold allowed the main chamber to be pumped out either directly by the diffusion pump via V_1 (see Figure 4, page 13) or indirectly through a cold trap via V_2. The indirect pumping was necessary to trap the organic vapors used in these experiments and to prevent them from contaminating the hydrocarbon oil of the forepumps.

The pure carrier gas pressures were measured by a standard mechanical gauge, model FA-145 (Wallace and Tiernan, Inc.). For a mixture of organic vapors with a carrier gas (at any temperature) a pressure sensing strain gauge was used, which was calibrated at each temperature to the Wallace and Tiernan gauge using pure N_2. The pressure sensing strain gauge was installed through the top plate of the chamber such that the

sensitive element edge was parallel with the lower edge of the chamber plate. The pressure sensing device is a low level, absolute transducer, model PA288TC-50-350 (Statham Instruments, Inc.), which has a diaphragm attached to a resistive unbounded strain gauge. The transducer unit is arranged in a conventional, balanced, four-active-element Wheatstone bridge. With voltage excitation, provided by a bridge balance unit, model 1-100DX, and power supply, model 15-200D (B and F Instruments, Inc.), the transducer provides an electrical output proportional to the applied pressure. The PA288 is a flush diaphragm transducer that is temperature compensated between 220° and +477° K., with a range of 0 to 50 p.s.i.a. and was specially selected to have a combined linearity and hysteresis of $\pm$ 0.25 per cent of full scale. The calibration factor used was 184.5 microvolts (open circuit) per volt per p.s.i. The readout of the transducer was done with a circular indicator, model 15601836-01-0 (Honeywell, Inc.), that has a span of 0 - 50 mV. and an indicator dial with a range of 0 - 2000 torr.

The small attaching gas pressures were measured with a high precision MKS baratron pressure meter (MKS Instruments, Inc.). This instrument consists of a 10 torr pressure head, model 77H-10, and a pressure indicator, model 77M-XR. The full scale of the pressure indicator can be set to correspond to various pressure ranges (0-3μ, 0-10μ, 0-30μ, 0-100μ, 0-300μ, 0-1000μ, 0-3000μ, and 0-10,000μ) which allowed measurements of the sample gas pressures to within a tenth of a micron. This

capacitance manometer is a differential pressure device and measures true pressure, regardless of the gas introduced. A vacuum was used as the reference pressure, i.e., the reference P_R side of the head was piped to the mounting flange of the diffusion pump. The pressure head was custom built for use up to a temperature of 477° K. It contained silicon embedded heater elements which were controlled by an Electro-Flex (Electro-Flex Heating, Inc.) temperature controller. The controller had a thermocouple readout so that the temperature of the MKS head could be controlled independently of the temperature of the chamber. A ten-turn potentiometer was installed in the MKS readout unit to allow the application of voltage bias to the pressure bridge for zero offset at temperatures higher than room temperature.

A number of Hastings thermocouple vacuum gauges, model VT-5 (range 0 to 100μ), were introduced at various parts of the system to monitor the reference side of the MKS pressure meter, or to indicate the pressure of the main chamber as well as other parts of the system, or to aid in the purification process.

Two carrier gases were used in these experiments: ethylene (C_2H_4) and nitrogen (N_2). High purity commercial nitrogen was obtained which needed no further purification. Ethylene (99.5 per cent purity, Matheson Company), however, had to be further purified as small amounts of impurities produce a marked error in the results.

A gas manifold system was designed for purifying the carrier gases and filling the chamber. The system contained two manifolds and was capable of handling two gases separately, but had a cross-over line so that all four cold traps could be placed in series if necessary. The cold traps were constructed of stainless steel and sealed with copper "O-rings" to allow high temperature bakeout. Ethylene was run through two cold traps and was well purified by fractional distillation. Stainless steel turnings were used in the cold traps to increase their efficiency. The fractional distillation was done at liquid nitrogen temperatures. A pressure gauge, a Hastings gauge, and two pressure relief valves were supplied to each manifold. The prepurified carrier gas was introduced slowly into the main chamber either from the top or the bottom through two needle valves.

III. ELECTRONICS AND DATA READOUT

The following instrumentation was used. Two regulated high voltage power supplies, a 1 - 10 kV., model 410A (John Fluke Manufacturing Company, Inc.), and a 0 - 1 kV., model 240 (Keithley Instruments, Inc.), were connected through filters to the emitter plate. Also, a 0.5 - 6 kV., model 408A (John Fluke Manufacturing Company, Inc.), power supply was used to supply high voltage to the gas discharge tube. A fourth 0.5 - 2.5 kV., model 2.5/10 uc (Electronics Research Associates), power supply provided the high voltage for the gas discharge xenon phototube.

The preamplifier used in these experiments was re-designed to reduce noise (see Figure 6 for circuitry), and the A-1D [Jordan and Bell (1947)] linear amplifier was modified as described by Hurst and Bortner (1958). An Oak Ridge National Laboratory single channel differential analyzer, model Q-1192, which has a motor-driven base line so that the "window" scans uniformly in time, was used. A display of the analyzer output on a 0.25 sec. recorder afforded a convenient method of pulse height measurement. Also, an Oak Ridge National Laboratory mercury relay pulse generator, model Q-1212D, was used for calibration purposes.

Figure 7a shows the circuit of the ultraviolet xenon flash light source, and Figure 7b shows the photodiode used for the drift velocity measurements to give $t = 0$ (see Chapter III).

A model 555 oscilloscope (Tektronix, Inc.) was used for the drift velocity measurements and a model 543 oscilloscope (Tektronix, Inc.) was used for observation of the pulses due to α-particles in the pulse height measurements. An Electronik class 15 (Honeywell, Inc.) multipoint recorder automatically recorded the thermocouple readings. Use was made of other electronics closely associated with heating control and thermocouples (see Section IV of this chapter).

The major problem encountered with this system of electronics was due to noise. The noise level must be kept to a minimum in order to have good accuracy in the measurements. Noise can result from poor

ORNL DWG. 65-11015

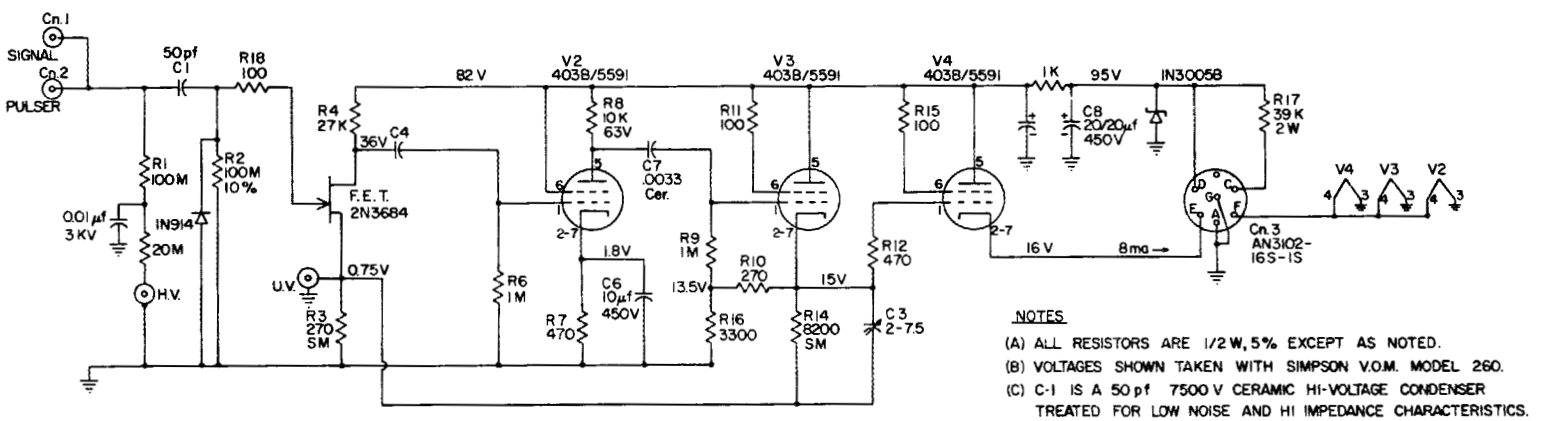

Figure 6. Circuit of preamplifier used in electron attachment studies.

ORNL DWG. 67-12402

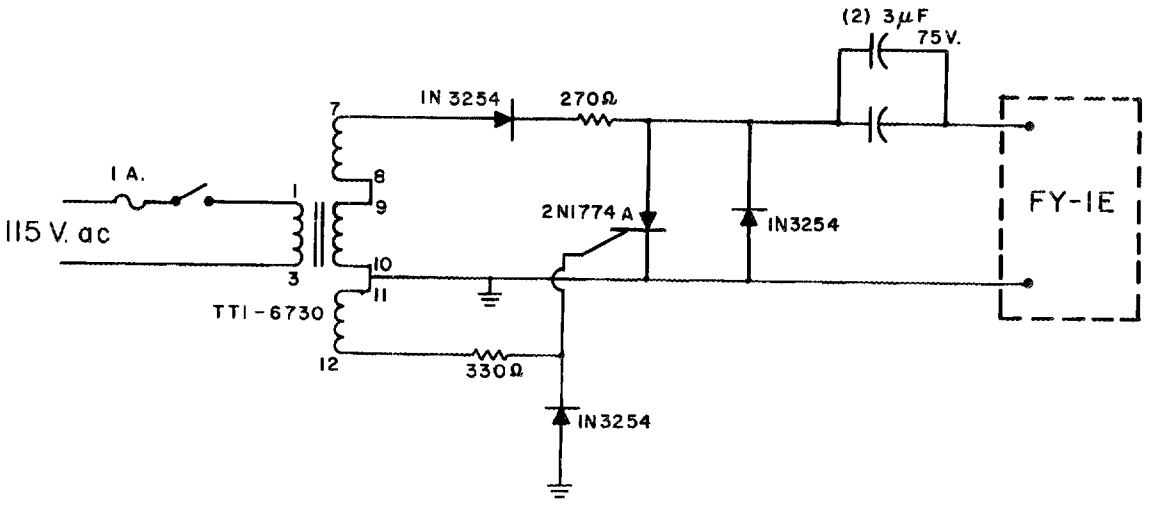

Figure 7. a) Ultraviolet xenon light source schematic.

Figure 7. b) Photodiode schematic.

engineering and construction: faulty components, hum, microphonics, and electromagnetic and electrostatic pickup from sources external to the measuring equipment. Another source of noise arises from fundamental properties of electron current: thermal motion of electrons in the detector load resistor, grid current, flicker effect and shot effect in the input tube.

The most obvious external source of noise is that arising from the 60-cycle AC and its harmonies (classified as a hum). To reduce hum, a DC power supply was used for the heater current in the preamplifier.

Microphonic noise may have a number of sources: tubes, signal-carrying wires, and the signal source (parallel-plate chamber) due to mechanical vibrations. Ruggedized tubes were selected as they are designed to minimize microphonic noise. Vibration of the chamber plates produced variation in the chamber's electrical capacitance; hence spurious noise was generated in the signal source itself. The entire apparatus was accordingly shock mounted from the floor to reduce mechanical pickup of vibrations in the building. The flow of the heating oil through the heating assembly was an additional source of microphonic noise. Most of this microphonic noise was coupled into the system by the first stage of the preamplifier. This effect was drastically reduced by changing the input tube of the preamplifier to a field effect transistor, FET. 2N3684 (Union Carbide Electronics).

Two techniques were applied to minimize the pickup of noise from outside the measuring equipment: (i) the shielding of cables and high impedance components, and (ii) the avoidance of multiple grounds. All cables were of the single-shield type, usually grounded at only one end. By grounding the shield at one end (the source end), noise currents could be avoided. It was also recognized that elimination of multiple grounds was necessary since potential differences might exist between them.

High impedance components are quite sensitive to external electrostatic and electromagnetic fields. Noise pickup in this case can best be avoided by keeping high impedance leads short and properly shielded.

The usual trial-and-error method of noise reduction proved valuable in constructing the circuits. The output of the amplifier was monitored with an oscilloscope while various configurations of grounding, shielding, lead placement, and external equipment were tried.

The characteristics of a low-noise operating tube usually are low transmittance (μ), high conductance (gm), and low grid current (Ig). A number of commercially available tubes exhibiting these characteristics were examined by Fairstein (1958). Among these are the 6AF4, 6T4, 6AJ5, 6AK5, 403B, and 12AF6. Two particularly suitable tubes, 6AK5 and 403B, were selected for the low-noise preamplifier and amplifier used in this experiment. A wide variation in μ, gm, and inherent noise level was found within tubes of the same type. Therefore, a number of tubes were

selected and each individually checked for gain, grid current, and low noise. The selected tubes were rotated to the various positions in the circuit. In this manner it was possible to maximize the gain of the preamplifier and minimize the noise level for given operating conditions.

In high temperature regions the electrical resistance among insulated circuit components can drop to one megohm or less, and gain of circuit components changes as a function of temperature. The preamplifier was located very close to the heated chamber and it was necessary to insulate this unit thermally from the chamber and cool it by flowing chilled compressed air across the circuit components.

IV. HEATING SYSTEM

Efforts were made to control the temperature within $\pm 1°$ K. in the main chamber over the temperature range (295° to 500° K.). We chose a flowing liquid system with accurate temperature control to provide the heating, and thermocouples to give the temperature information inside the chamber. Several systems were studied, and thermocouples with multipoint recorder readout were selected due to their many advantages which include good speed of response, wide range of measurement, relatively small size, simplicity, ease of installation, absence of self heating and lower cost. The thermocouples used were "Ceramo" assemblies (Thermo Electric Company, Inc.), types 5E1511A and 5E1541A. The sheath material

was stainless steel with an adjustable bushing terminating in a welded hot junction. The wires were chromel-constantan since they generate the highest e.m.f. per degree change in temperature of other standard thermocouples, and their accuracy holds for a longer period of time. Because of the wide variation of the thermoelectric characteristics of wires which are nominally identically, calibration of the thermocouples was essential. The problem is made simpler when the thermocouples are incorporated into a reference junction with permanently embedded thermocouples. The reference junction was a model 2450 (Acromag, Inc.) with a reference temperature of 273° K.

The readout of the thermocouples was done by a strip chart recorder, model 15304836 (Honeywell, Inc.) syncroprint, 12 point. This recorder has adjustable span (1 to 21 mV.) and adjustable suppression ($\pm$ 20 mV.), giving the capability of nulling out any part of a thermocouple signal and then expanding the remaining signal over a more sensitive scale. Therefore, we could expand and record any two to three degrees of temperature over the entire temperature range.

The reference junction was mounted inside the recorder case, and all internal connections to the recorder terminal board and amplifier were made with copper wire. Before calibration of the thermocouples, the recorder was carefully balanced and calibrated on all scales with a Rubicon

potentiometer which was then wired to the recorder, allowing a check at any time of the recorder settings and thermocouple output.

The thermocouples were wired to the recorder and the calibration of the reference junction was checked by taking three of the thermocouples to 273° K. in an ice bath. After compensating for the thermal e. m. f. generated at the terminal board of the recorder, the output of the reference junction for all three thermocouples was less than five microvolts at 273° K. The calibration of all eight thermocouples was then done at three points: the ice point of water, the boiling point of water, and the boiling point of naphthalene. Then a plot of ΔE, the difference between the observed and standard e. m. f., against the standard e. m. f. was made.

Since our interest was to detect small changes in temperature over the region of 293° to 500° K., the thermocouples were placed in a sand bath, in a temperature-controlled oven with a mercury thermometer, and a strip chart run for all eight thermocouples at ten degree intervals. These points were also plotted as ΔT against the thermometer temperature as the standard. The thermocouples were then ready for installation. The millivolts to temperature conversions were taken from Adams and Davisson (1965).

A heating system with close temperature control and a minimum temperature gradient across the chamber was necessary to eliminate gas convection currents once thermal equilibrium was established. It was

decided that a flowing liquid would be the means of heat transfer. The walls of the chamber would act like a thermal shroud to the gases. The bottom and top of the main chamber were well insulated and heated by conduction from the walls and by electric tape heaters when necessary.

The major components of the heating system are shown in Figure 8. They include the chamber, cooling coil, pump, heat transfer fluid, heater, and controller. The chamber has been described previously. For purposes of heat and flow calculations, the copper helix between the walls was considered to form a rectangular duct 1.5 in. high, 0.5 in. wide, and 142 in. long. Since the helix clears the outer wall by only 0.031 in., this is probably a good approximation.

The cooling coil was necessary to allow temperatures below about 350° K. due to friction heating of the oil. The coil was 0.375 in. copper tube silver soldered to the outside of a 2 in. schedule 10 stainless steel tube that carries the heating fluid. This is encased by a 3 in. schedule 10 stainless steel tube and capped at both ends.

The pump was a centrifugal, "canned" rotor type, model 1001 (Integral Motor Pump Corporation). It has a 1.5 H.P. motor operating on 440 volts. The impeller diameter is 4-7/8 in. The motor windings were class H, gaskets were teflon, and the fluid being pumped served as the coolent.

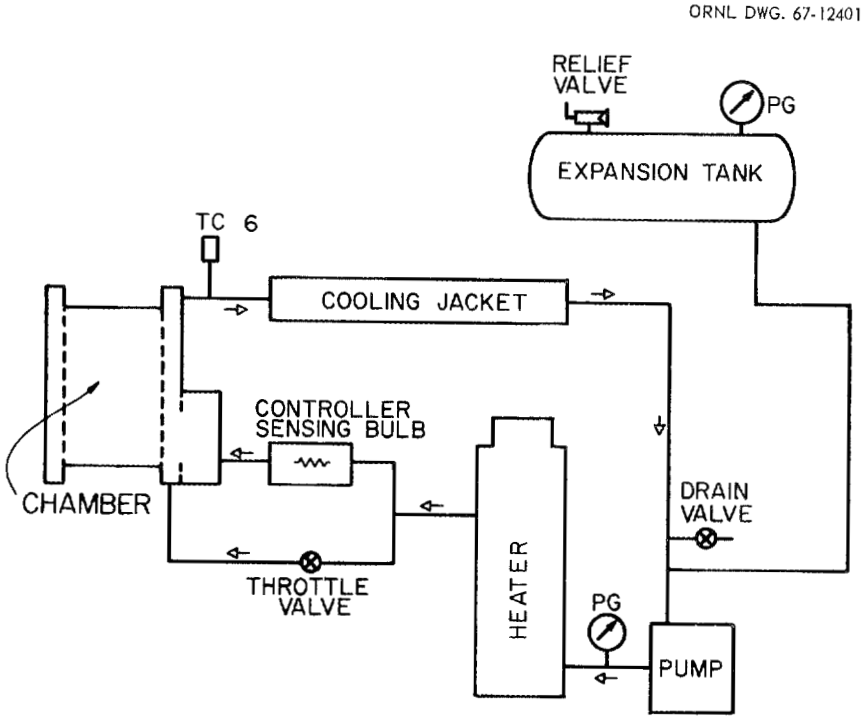

Figure 8. Diagram of heating system.

The heat transfer fluid was Dow Corning 200 (Dow Corning Corporation) with 20 centistoke viscosity at 298° K. This fluid has some characteristics particularly favorable to our experiment such as relatively flat viscosity-temperature slope (i.e., 20 centistoke at 298° K. to 2.7 centistoke at 480° K.), low vapor pressure, high flash point (510° K. at 20 centistoke), nontoxicity, chemical inertness, and a specific heat at 373° K. equal to 0.353 cal./gm./° K. In many cases the heat transfer information on fluids is largely empirical. We found the "Dowtherm A and E Handbook," published by the Dow Chemical Company of Midland, Michigan, very helpful.

The heater unit was a Chromalox oil circulation heater, model NWHO-3301 (Edwin L. Wiegard Company). It had a total output of 3 kilowatts, 1000 watts from each of three heaters, and operated on 115 volts AC, single phase, with a watt density of 22 watts/sq. in. The heater unit had a type AR thermostat that had a range of 360° to 533° K. The wiring of the heaters is shown in Figure 9. This wiring allowed maximum flexibility and control without heavy current loading on the controller.

The oil temperature controller was a Power-O-Matic 60, model RA1A-6 (Blue M Electric Company). It was a saturable reactor, proportioning control system with a maximum output of 1750 watts. The temperature range covered was 273° to 477° K., and the temperature was continuously variable. The temperature sensing element was a filled

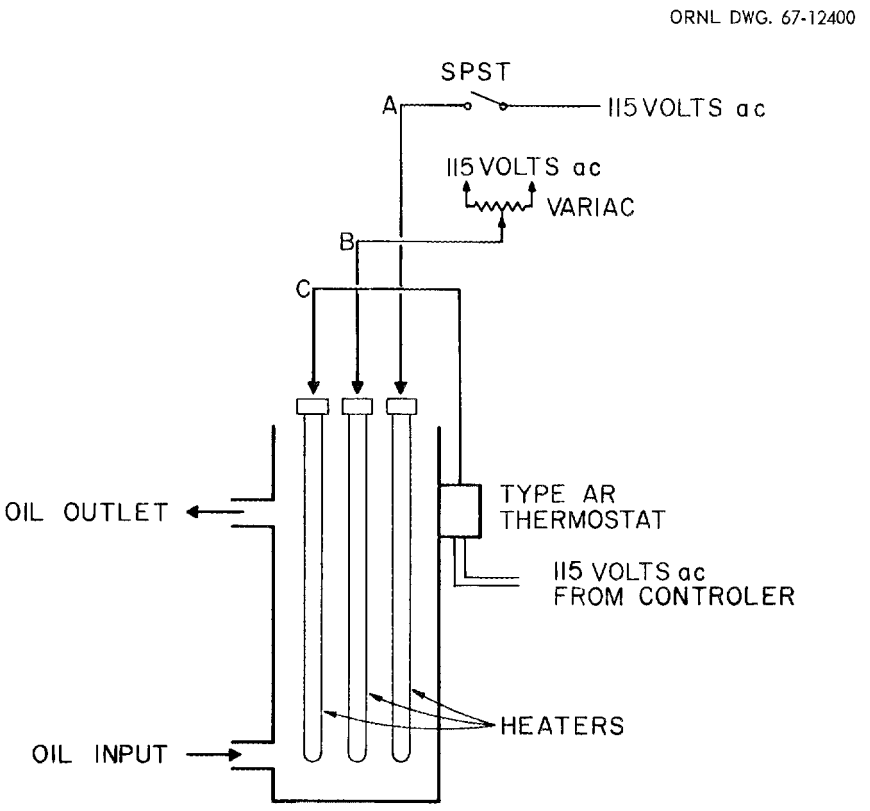

Figure 9. Diagram of heater wiring.

sensing bulb connected through capillary tubing to hydraulic bellows. The bellows plunger contacted the movable armature of an inductor coil assembly which controlled the wattage to the saturable reactor. This in turn controlled the output voltage applied to the control heater. The system was inherently accurate with control repeatability of 0.5 per cent of the scale range, required no compensation for ambient temperature effects, and had excellent dynamic response. The only problem incurred was one of getting the four foot length of the sensing bulb into the oil flow. This was accomplished by the construction of a coupling flange to which four stainless steel rods were welded. The sensing bulb was inserted through the side of the flange with a compression gasket and coiled around the four support rods. The bulb was held in place by soldering small holding wires around the bulb and support rods. A housing was built and the sensing bulb assembly inserted. The entire assembly was then placed in the oil flow system just before the chamber and sealed with copper gaskets (Figure 8, page 32).

The entire heating assembly was then covered with two layers of insulation. The first layer was flexible Min-K, type P-38 (Johns-Manville), and the second layer was Cerafelt, type 600 (Johns-Manville). The insulation was held in place by aluminum reflective tape.

CHAPTER III

FUNCTIONING OF THE APPARATUS AND EXPERIMENTAL PROCEDURE

The Jordan and Bell (1947) linear pulse amplifier was modified [as in Bortner and Hurst (1958)] so that in the long time constant position it would give a pulse shape like that described in Equation (7) with $t_1 = 20$ microseconds. The response of the amplifier used to a step function pulse is shown in Figure 10. With $t_1 = 20$ microseconds, the agreement with the idealized response given by Equation (7) is good up to approximately 60 microseconds. Deviation from the idealized response will not, however, effect the pulse height, provided the amplifier output pulse peaks in less than about 60 microseconds.

The dependence of pulse height on τ_o/t_1 was checked experimentally using pure nitrogen and pure ethylene and found to be in agreement with the theoretical expression given in Chapter I. The procedure for measuring pulse heights was identical to that of Bortner and Hurst (1958). At elevated temperatures the shape of the pulse height versus E/P curves remained unchanged but an overall decrease in the pulse height was observed with increasing temperature.

Before each set of measurements the chamber was heated for eight hours and then flushed with the carrier gas. The outgassing rate

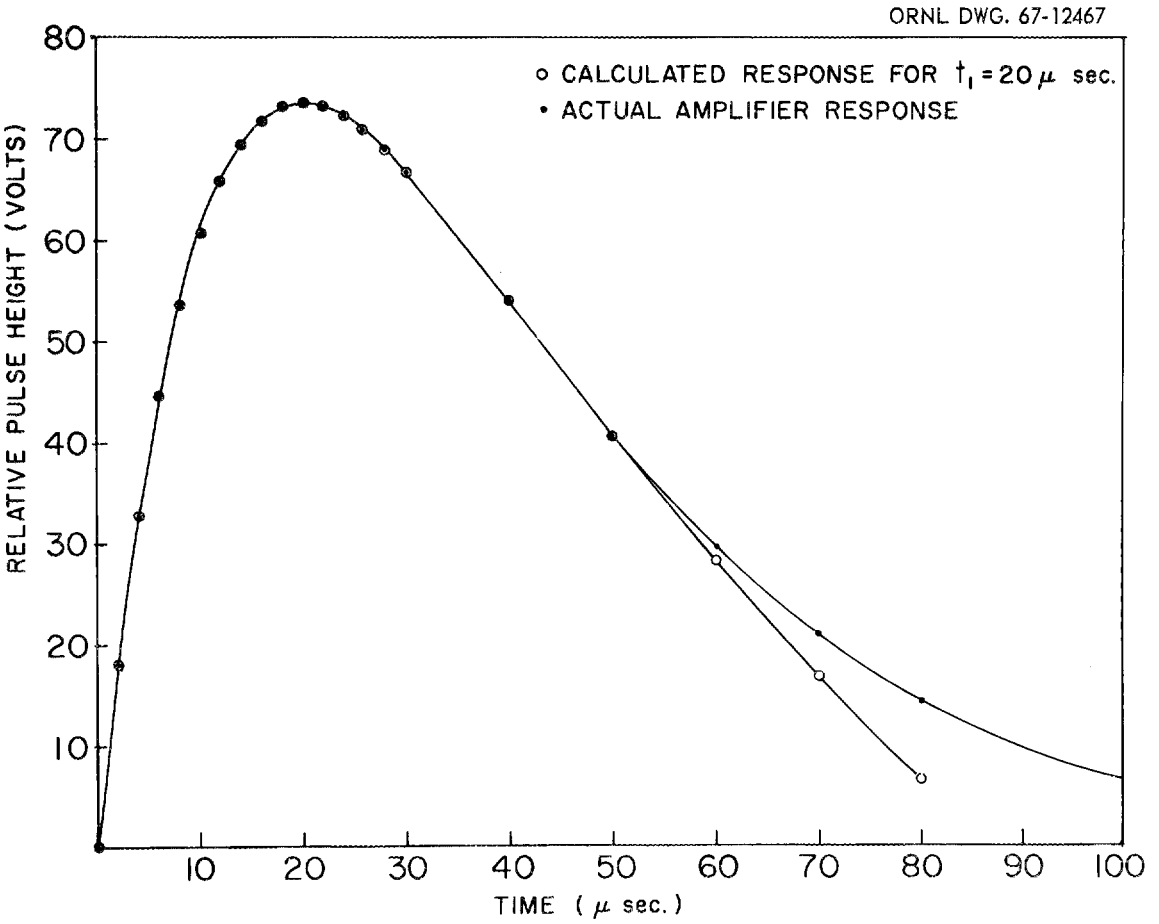

Figure 10. Measured response of the linear amplifier.

was measured, and the pressure devices were calibrated with pure N_2. Then the thermocouple readout was checked for zero shift, and the electronics calibrated.

A new experimental procedure for measuring drift velocities was developed and improved accuracy was achieved over the old method [Bortner, Hurst and Stone (1957), Christophorou, Hurst, and Hadjiantoniou (1966)]. The ultraviolet light emitted by the pulsed xenon flash tube (Figure 7a, page 25) passes through the quartz window and strikes the center of the emitter plate EM (Figure 3, page 12), releasing a number of photoelectrons. These electrons quickly come into equilibrium with the gas, and because of the applied electric field they travel the drift space EM-C and ultimately trigger the gas discharge tube G. M. A simple type of electronic quenching, consisting of a 100 megohm load resistor in the supply current, was used to prevent multiple pulsing and continuous discharge. The ultraviolet pulse which generates the electron swarm also triggers the photodiode (Figure 7b, page 25). The photodiode output pulse was fed to the preamplifier (Figure 6, page 24), to the A-1 amplifier (operated at 2 mc. bandwidth), and viewed with a Tektronix 555 oscilloscope. At some time Δt, after the display of the photodiode, the pulse from the gas discharge tube was also seen on the oscilloscope. The time lapse Δt between the two pulses is the drift time of the electrons and is of the order of microseconds.

To improve accuracy in the Δt measurements the following procedure was developed. The output from the amplifier was connected to both the external trigger position on a type 21 time-base unit of the 555 oscilloscope and to the input of a continuously variable time delay network, type 2011 (Advance Electronics Company, Inc.). The delay line contained an amplifier stage so the signal was not greatly reduced. The output of the delay line was applied to two type L input units in the 555.

The time delay of the variable delay and the sweep times of the 555 were checked and calibrated by means of a crystal generator.

With the A time base trigger level in normal and the trigger source control in external, the sweep of the A channel was triggered on the leading edge of the photodiode signal. By monitoring the signal, the trigger level could be set just above the noise level on the start of the photodiode pulse.

The inputs to the A and B channels could be delayed and displayed some time after the A channel sweep started. The usual procedure was to delay the inputs an amount equal to the setting of the A channel time per centimeter control which placed the start of the photodiode pulse exactly on the one centimeter grid line. When the B channel sweep function switch was placed in the "sweeps once for each A delayed trigger" position, a brightened portion of the A channel trace was clearly visible, and the brightened portion of the A trace was displayed on the B channel. By

adjusting the B channel time per centimeter control, the brightened area could be made to cover only a small portion of the A channel trace.

Using the delayed trigger control, the start of the brightened portion of the trace could be positioned at the start of the photodiode pulse and the setting of the control recorded. Turning the delayed trigger control positioned the brightened portion of the trace on the start of the G. M. pulse, and the setting of the control was recorded. By subtracting the first setting from the second and multiplying the result by the setting of the A channel time per centimeter control, the time interval between the two pulses was obtained. Measurement of the time interval was dependent only on the calibration of the scope and the linearity of the delayed trigger control, which was $\pm$ 0.1 per cent.

This was a simple way of obtaining the time interval Δt, and it gave reasonably accurate results. The use of the delay line eliminated error in selecting the exact start of the photodiode pulse.

The results are consistently within 0.5 per cent of results taken with much more elaborate methods of time measurement [Pack and Phelps (1961), Parks and Hurst (1965)].

CHAPTER IV

RESULTS AND DISCUSSION

Pulse heights and electron drift velocities were measured for the carrier gases nitrogen and ethylene at various temperatures ($298° \leq T \leq 473°$ K.). For pulse heights and drift velocities taken at temperatures higher than 298° K., E/P was normalized to P_{T_1} ($T_1 = 298°$ K.), i.e., $P_{T_2} = P_{T_1} (T_2/T_1)$, assuming an ideal gas behavior. When the changes in w with temperature are considered, the overall shape of the pulse height versus E/P curve for both carrier gases (N_2 and C_2H_4) remains unchanged in the temperature range studied. However, the absolute magnitude of the pulse height decreased slightly with increasing temperature. This, in part, may be due to changes in the C to G.R. (Figure 2, page 7) capacitance.

I. ELECTRON ATTACHMENT TO SF_6

SF_6 attaches electrons very strongly at thermal electron energies, and thus very low pressures of SF_6 have to be introduced into the ionization chamber in order to get any signal. Such low pressures ($< \sim 0.1$ micron) are difficult to measure, especially at high temperatures where a small outgassing rate becomes a major problem. An expansion technique was used in

which a few torr of SF_6 were measured with a Wallace and Tiernan gauge in a well-defined volume, and subsequently expanded into another tank of known volume. There the SF_6 was mixed with the carrier gas (ethylene) to a pressure of approximately 1000 torr. Known quantities of this mixture were then introduced into the ionization chamber through a solenoid valve of measured volume. Therefore, the amount of SF_6 in the ionization chamber was known from the volume ratios and from the amount of SF_6 prior to expansion. During measurements at higher temperatures no effects due to outgassing were detected.

The absolute rate of electron attachment was determined at low values of E/P (≤ 0.1 volt cm.$^{-1}$ torr^{-1}) where the energy distribution of electrons in the swarm is thermal [Christophorou et al. (1965)]. For this E/P region (≤ 0.1) a constant rate of attachment equal to 1.24×10^9 sec.$^{-1} \cdot$ torr^{-1} was measured. This value is the average of more than ten runs. The results were consistent and reproducible to within $\pm$ 15 per cent. The attachment rates decreased slightly for $E/P > 0.1$. Our value of the thermal attachment rate in SF_6 is an order of magnitude smaller than the recent value obtained from a microwave technique by Mahan and Young (1966).

The attachment rate was independent of the total pressure ($250 \leq P_{total} \leq 800$ torr). Complete stabilization of SF_6^{-*} is reasonable to assume in view of the long lifetime of SF_6^{-*}, approximately 25 microseconds

[Compton et al. (1966)], and the high pressures employed. (For these pressures, approximately 10^6 collisions occur within the lifetime of SF_6^{-*}.) Attachment rates measured under these conditions are thus representative of the rate of forward reactions and are not complicated by reverse processes.

II. TEMPERATURE DEPENDENCE OF THE ATTACHMENT RATES IN SF_6

The temperature dependence of the absolute rates of electron attachment in SF_6 was also investigated. The attachment rate, αw, is given by

$$\alpha w = N \int_0^\infty v \sigma_c(v) f(v) dv \tag{12}$$

where N is the number of SF_6 molecules per torr at 300° K., $\sigma_c(v)$ is the attachment cross section as a function of electron velocity, and

$$f(v) dv = (m/2\pi kT)^{3/2} \exp[-(mv^2/2kT)] 4\pi v^2 dv .$$

From Figure 11 we conclude that αw is temperature independent over the range 298° to 418° K. A cross section which is inversely proportional to the electron velocity, v, i.e.,

$$\sigma_c(v) = A/v , \tag{13}$$

is consistent with a constant αw in Equation (12). For comparison with

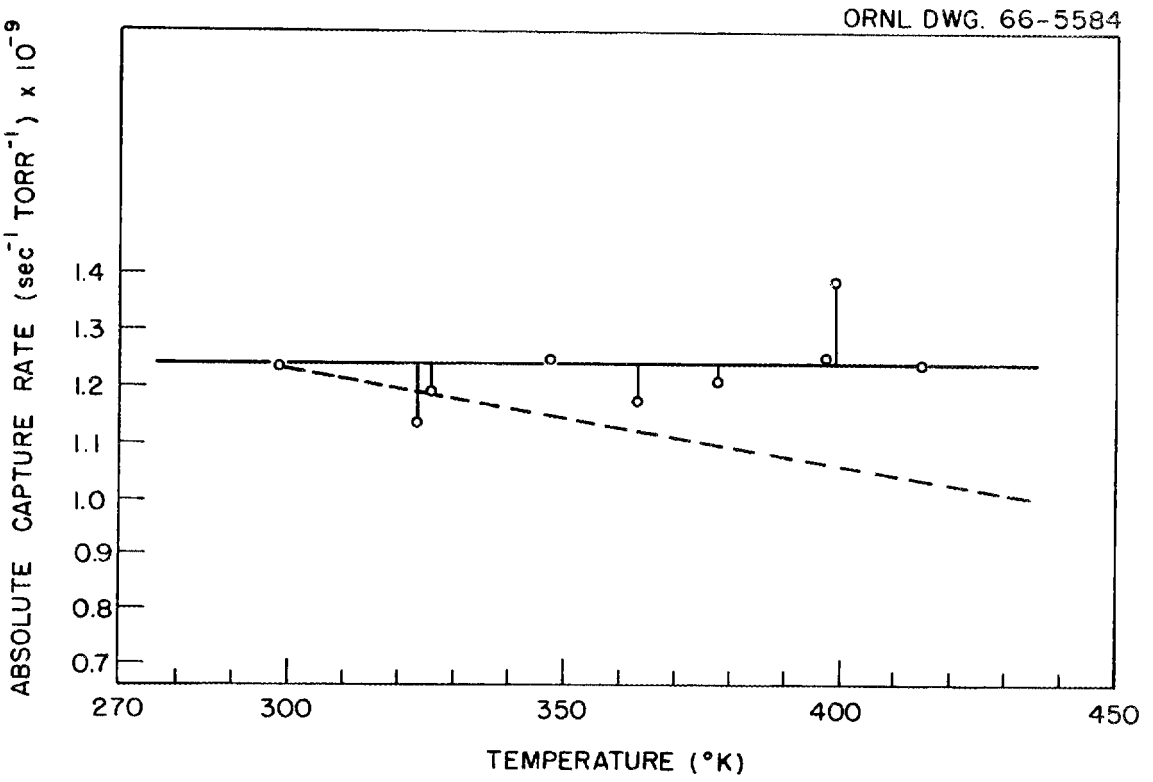

Figure 11. Temperature dependence of the electron attachment rates in SF_6.

the experimental data we also plotted (Figure 11) the temperature dependence of αw (broken line) which would have been observed had $\sigma_c(v)$ been inversely proportional to the square of the electron velocity. The velocity dependence of the electron attachment cross section has a theoretical basis and is analogous to the v^{-1} absorption law for low-energy neutrons in nuclear physics [Blatt and Weisskopf (1963)].

A physical foundation for the v^{-1} law is recognized from the fact that the cross section is a product of two factors, the effective area for attachment and the probability of encounter. Since the effective area for attachment is proportional to the square of the deBroglie wavelength and the probability of encounter varies in proportion to the density of momentum states, the attachment cross section is consequently proportional to v^{-1}.

From Equations (12) and (13), the constant A for SF_6 is calculated to be 3.83×10^{-8} cm.^{3} sec.$^{-1}$. Using this value and the average velocity $\bar{v}$ of a thermal electron [$\bar{v} = 1.07 \times 10^7$ cm./sec. at 300° K.], we calculated an average attachment cross section $\bar{\sigma}$ equal to 3.6×10^{-15} cm.^{2}. Table I gives a summary of the reported values on the attachment cross section of SF_6 at very low energies. Our value is comparable with those of total ionization experiments but is in disagreement with the two widely differing values reported by the microwave technique. The comparison of the attachment cross sections in Table I is complicated, however, by the

TABLE I

ATTACHMENT CROSS SECTIONS FOR SF_6^-

σ_c (cm.^{2})	Method
3.6×10^{-15} (average)	Swarm (present work)
1.3×10^{-15} (at maximum)	Total ionization[a]
2.4×10^{-16} (at maximum)	Total ionization[b]
5.7×10^{-16} (at maximum)	Total ionization[c]
$\sim 10^{-15}$ (at maximum)	Mass spectrometer[d]
2.6×10^{-14} (average)	Microwave[e]
3×10^{-20} (average)	Microwave[f]
3.6×10^{-14}	$\pi\lambda\!\!\!^{-2}$ (λ for $\bar{v}$)

[a] R. K. Asundi and J. D. Craggs, Proc. Phys. Soc. (London) 83, 611 (1964).

[b] D. Rapp and D. D. Briglia, J. Chem. Phys. 43, 1480 (1965).

[c] N. S. Buchel'nikova, Soviet Phys.—JETP 35, 783 (1959) [Zh. Eksperim. i Teor. Fiz. 35, 1119 (1959)].

[d] W. M. Hickam and R. E. Fox, J. Chem. Phys. 25, 642 (1956).

[e] B. H. Mahan and C. E. Young, J. Chem. Phys. 44, 2192 (1966).

[f] J. B. Hasted and S. Beg, Brit. J. Appl. Phys. 16, 74 (1965).

very sharp resonance peak involved (each value represents an average which depends on the experimental condition).

III. ELECTRON DRIFT VELOCITIES IN NITROGEN AND ETHYLENE AS A FUNCTION OF TEMPERATURE

Drift velocities in nitrogen and ethylene were measured for temperatures ranging from 298° to 473° K. The results are presented in Tables II and III and are plotted as a function of E/P (P = 400 torr) for the temperatures 298° and 473° K. in Figures 12 and 13.

Drift Velocities in Nitrogen

The drift velocities in nitrogen were found to decrease with temperature (see Table II and Figure 12). Such behavior was observed previously by Pack and Phelps (1961) and by Lowke (1963). However, the data reported by these authors were for only a few temperature values. (Lowke's data were reported for 75° and 293° K., while Pack and Phelps reported w values for 77°, 195°, 300°, and 375° K.) It is worth noting that while Pack and Phelps (1961) did not observe any temperature dependence of w for $E/P \geq 0.1$, our results show that there exists a T dependence of w for E/P up to 1.8. The decrease in w with increasing T may be due to an increase in the average electron agitation energy.

TABLE II

ELECTRON SWARM DRIFT VELOCITIES (CENTIMETERS PER MICROSECOND) IN NITROGEN AT VARIOUS TEMPERATURES

E/P	298° K	313° K.	323° K.	333° K.	348° K.	388° K.	403° K.	438° K.	473° K.
1.8	1.14	1.14	1.111	1.030	1.124	1.098	1.090	1.074	1.065
1.6	1.045	1.04	1.016	1.025	1.034	1.010	1.008	0.989	0.987
1.4	0.940	0.943	0.928	0.934	0.927	0.914	0.908	0.891	0.890
1.2	0.858	0.850	0.843	0.840	0.837	0.830	0.825	0.807	0.805
1.0	0.760	0.765	0.737	0.743	0.737	0.734	0.731	0.722	0.720
0.8	0.662	0.665	0.642	0.650	0.649	0.643	0.635	0.629	0.625
0.6	0.565	0.573	0.553	0.557	0.557	0.552	0.546	0.547	0.540
0.4	0.474	0.481	0.469	0.468	0.467	0.465	0.461	0.461	0.456
0.2	0.375	0.372	0.370	0.370	0.361	0.361	0.361	0.369	0.360
0.1	0.311	0.310	0.309	0.305	0.302	0.299	0.300	0.297	0.299
0.08	0.296	0.295	0.296	0.292	0.284	0.281	0.280	0.278	0.275
0.06	0.281	0.278	0.278	0.275	0.266	0.263	0.263	0.252	0.248
0.04	0.254	0.253	0.248	0.245	0.234	0.229	0.215	0.209	0.190
0.02	0.180	0.176	0.171	0.168	0.159	0.152	0.141	0.133	0.117
0.01	0.106	0.104	0.104	0.102	0.097	0.091	0.085	-----	-----
0.005	0.057	0.057	0.057	0.055	0.050	0.048	0.041	-----	-----

TABLE III

ELECTRON SWARM DRIFT VELOCITIES (CENTIMETERS PER MICROSECOND) IN ETHYLENE AT VARIOUS TEMPERATURES

E/P	298° K.	313° K.	323° K.	333° K.	348° K.	388° K.	403° K.	438° K.	473° K.
1.8	5.63	5.62	5.625	5.62	5.63	5.63	5.63	5.63	5.63
1.6	5.42	5.40	5.39	5.39	5.39	5.39	5.41	5.39	5.38
1.4	5.17	5.16	5.17	5.17	5.17	5.15	5.16	5.15	5.15
1.2	4.88	4.88	4.49	4.49	4.49	4.91	4.86	4.90	4.87
1.0	4.57	4.57	4.57	4.57	4.59	4.56	4.63	4.58	4.58
0.8	4.19	4.16	4.15	4.16	4.18	4.15	4.17	4.15	4.13
0.6	3.66	3.67	3.66	3.65	3.63	3.64	3.58	3.63	3.62
0.4	2.86	2.85	2.88	2.87	2.91	2.87	2.77	2.83	2.83
0.2	1.70	1.70	1.68	1.68	1.62	1.57	1.52	1.54	1.50
0.1	0.932	0.931	0.927	0.926	0.900	0.837	0.829	0.813	0.775
0.08	0.756	0.754	0.748	0.737	0.720	0.676	0.664	0.625	0.621
0.06	0.575	0.573	0.565	0.555	0.545	0.511	0.502	0.496	0.452
0.04	0.387	0.384	0.381	0.376	0.368	0.347	0.342	0.343	0.330
0.02	0.196	0.194	0.191	0.188	0.186	0.174	0.170	0.170	0.162
0.01	0.100	0.100	0.099	0.098	0.095	0.089	0.088	0.084	0.078
0.005	0.050	0.050	0.050	0.051	0.048	0.045	0.045	0.045	0.043

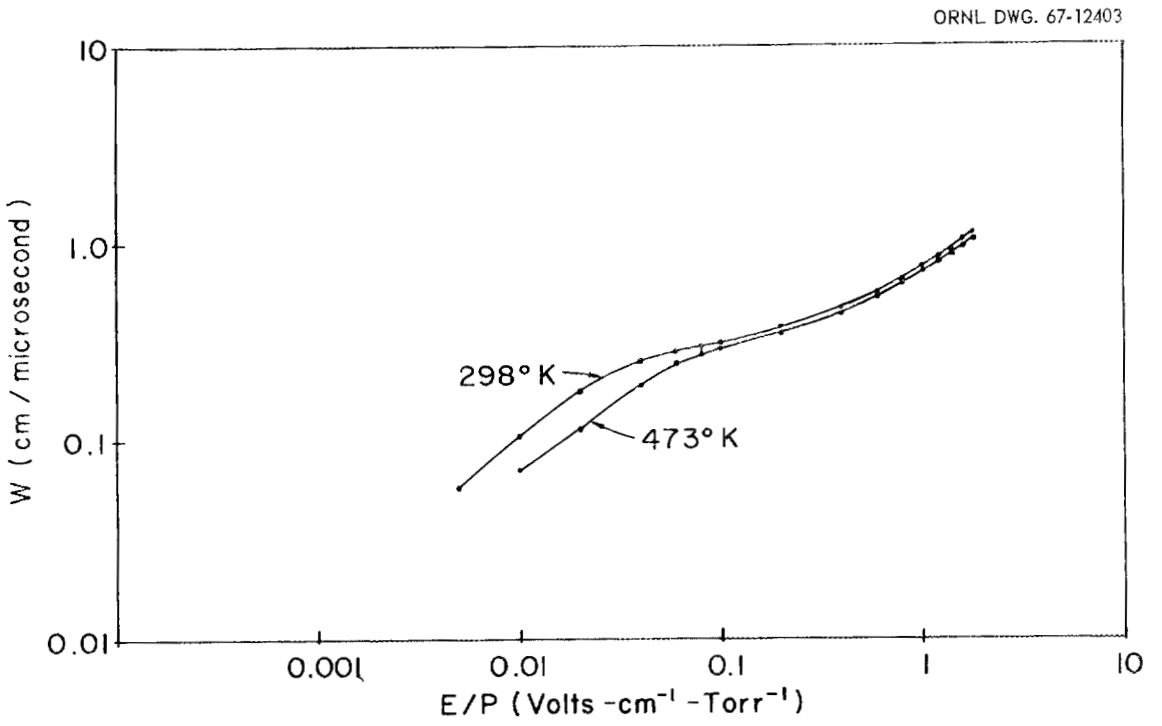

Figure 12. Electron drift velocities in nitrogen versus E/P for 298° and 473° K.

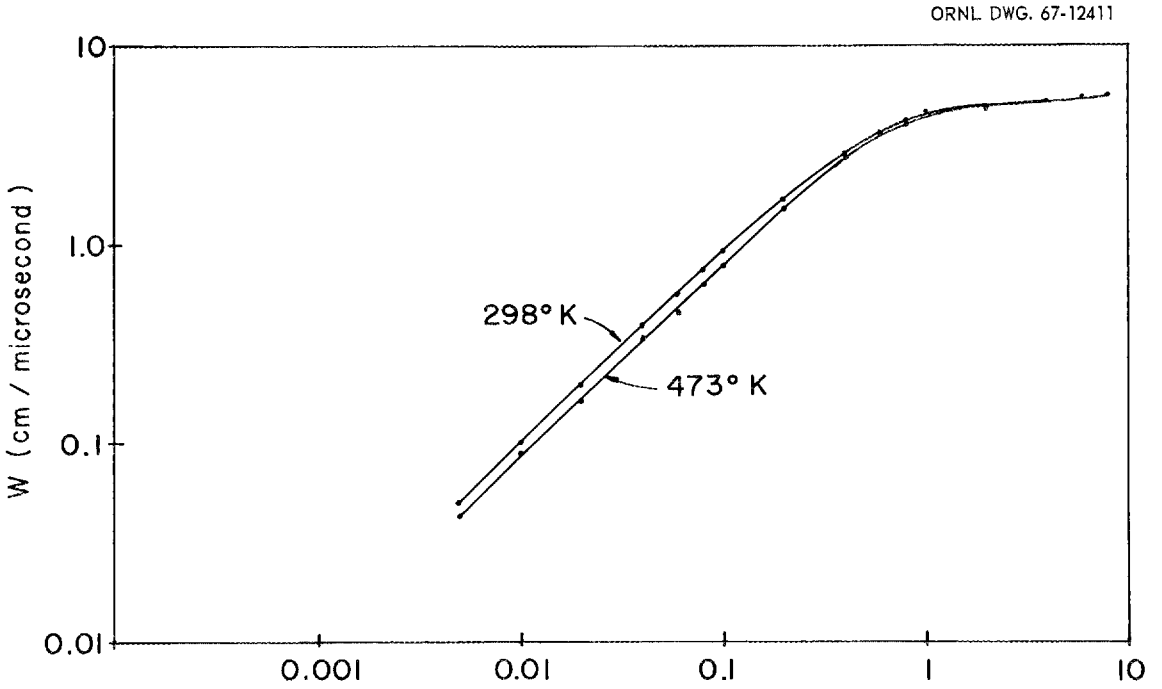

Figure 13. Electron drift velocities in ethylene versus E/P for 298° and 473° K.

Drift Velocities in Ethylene

The drift velocities in C_2H_4 were found to decrease with temperature up to at least an $E/P = 0.4$ as seen in Table III, page 49, and Figure 13. More recently Hamilton and Stockdale (1967) have confirmed our results on the T dependence of w in C_2H_4.

The change in w with increasing T for both gases is not due to possible outgassing at higher T. If the w changes were due to electron attaching polar impurities, pulse height changes would be observed and no such changes were detected. This, however, does not exclude the possibility of polar non-attaching impurities. Nevertheless, the amount of impurity necessary to cause the observed w changes would be such as to make this highly improbable.

IV. VELOCITY DEPENDENCE AND MAGNITUDE OF THE CROSS SECTION FOR MOMENTUM TRANSFER IN ETHYLENE

We shall now make use of the observed dependence of w on T in an attempt to deduce both the velocity dependence and the magnitude of the cross section for electron momentum transfer in ethylene. In the region of low E/P ($E/P \leq 0.1$), where the applied field does not disturb appreciably the electron energy distribution, the electron energy distribution is assumed to be Maxwellian [Stockdale and Hurst (1964), Christophorou et al. (1965)]. Thus, we may write [Allis (1956)]

$$w = -\frac{4\pi}{3}\frac{e}{mN}\frac{E}{P}\int_0^\infty \frac{v^2}{\sigma(v)}\frac{df_o}{dv}\,dv \tag{14}$$

where

$$f_o(v) = \left(\frac{m}{2\pi kT}\right)^{3/2} e^{-mv^2/2kT} . \tag{15}$$

In these equations E/P is the pressure reduced electric field; v, m, and e are the electron velocity, mass, and charge, respectively. We shall take N to be the number of gas molecules per cm.^{3} when $P = 1$ torr and when $T = 298°$ K.

Let us now assume that the cross section for momentum transfer is expressed in powers of velocity, i.e.,

$$\sigma(v, \alpha) = \frac{A_\alpha}{v^\alpha} \tag{16}$$

where A_α is a constant depending only on α. We then may show that

$$w = \frac{4}{3(2\pi)^{\frac{1}{2}}}\frac{e}{mN}\frac{E}{P}\frac{2^{\alpha/2}}{A_\alpha}\Gamma\left(\frac{\alpha}{2}+2\right)\left(\frac{m}{kT}\right)^{\frac{1}{2}(1-\alpha)} \tag{17}$$

where $\Gamma(x)$ is the gamma function of x, and α can be any quantity greater than -4. The temperature dependence of w follows from Equation (17). Some special cases are given in Table IV. In the table A_α is a constant independent of E/P and T. The assumption of a single

TABLE IV

TEMPERATURE DEPENDENCE OF w(T)
FOR VARIOUS VALUES OF α

α	$\sigma(v, \alpha)$	$w(T)$
-2	$A_{-2} v^2$	$K_{-2} E/P\, T^{-3/2}$
-1	$A_{-1} v$	$K_{-1} E/P\, T^{-1}$
0	A_0	$K_0 E/P\, T^{-1/2}$
1	$A_1 v^{-1}$	$K_1 E/P$
2	$A_2 v^{-2}$	$K_2 E/P\, T^{1/2}$
3	$A_3 v^{-3}$	$K_3 E/P\, T$

power of velocity leads to a unique temperature dependence, as illustrated in Table IV.

Our results for the drift velocity in pure ethylene were compared with Equation (17) for E/P ranging from 0.01 to 0.10 volt $cm.^{-1}$ $torr^{-1}$ and for T ranging from 298° to 473° K. It was found that when $\alpha = 0$ a good fit to Equation (17) was obtained with a constant cross section (σ_E) equal to $\sigma_E = A_o^E = (4.37 \pm 0.26) \times 10^{-16}$ $cm.^2$, where the $\pm$ represents extreme variations in 42 data points. This is shown in Figure 14. Attempts to fit the results to other values of α obviously fail, hence we conclude that the cross section for momentum transfer in ethylene is independent of velocity in the range of electron energies between approximately 0.01 eV. and 0.1 eV. and has the value $(4.37 \pm 0.26) \times 10^{-16}$ $cm.^2$.

Christophorou et al. (1966) have used this finding to further analyze the drift velocity data for mixtures of polar molecules with ethylene and to derive cross sections for momentum transfer for polar molecules mixed with ethylene. Further, Stockdale, Christophorou, Turner, and Anderson (1967) have used this finding to derive information for the minimum electric dipole moment necessary to bind an electron to a polar molecule from an analysis of drift velocity data on mixtures of polar molecules with ethylene.

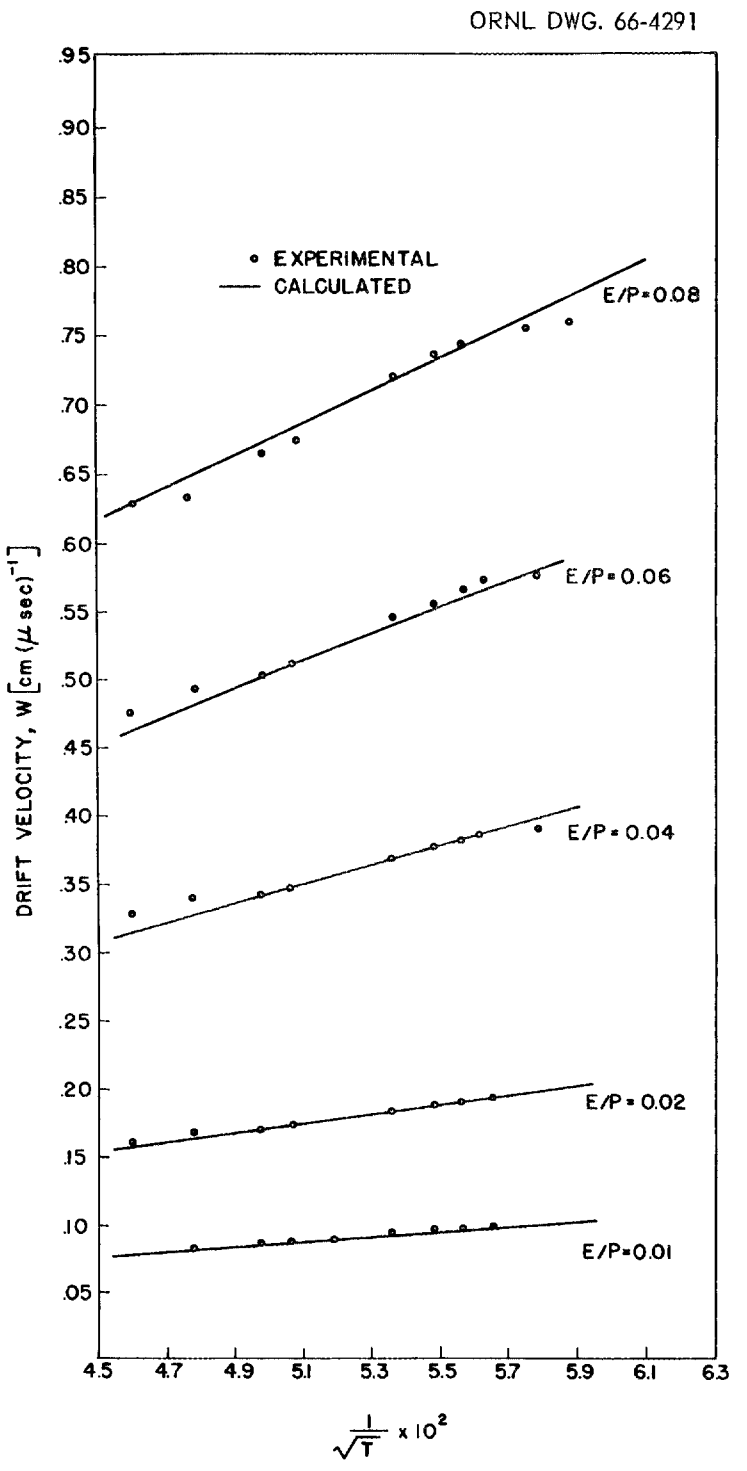

Figure 14. Experimental and calculated values of w (for $\alpha = 0$) as a function of temperature for various E/P.

CHAPTER V

CONCLUSIONS

An apparatus has been built for the study of electron swarm drift velocities and electron attachment to molecules for temperatures ranging from 273° to 473° K. The apparatus has been used for the study of electron attachment to SF_6 at thermal energies. The thermal rate of attachment to SF_6 has been measured in the temperature range 273° to 473° K. and found to be temperature independent. Thus it has been concluded that the electron attachment cross section for SF_6 at thermal energies varies inversely with the electron velocity when the attachment cross section is assumed to be expressed in powers of the electron velocity.

Electron drift velocities in nitrogen and ethylene have also been measured over the temperature range 273° to 473° K. and found to decrease as temperature increases. An analysis of the temperature dependence of the w data in C_2H_4 yielded a velocity independent cross section for momentum transfer equal to $(4.37 \pm 0.26) \times 10^{-16}$ cm.^{2} at thermal energies. This finding has been further used to obtain information on the scattering of thermal electrons from polar molecules.

BIBLIOGRAPHY

Adams, R. K., and E. G. Davisson, "Smoothed Thermocouple Tables of Extended Significance (° C)," Oak Ridge National Laboratory Report ORNL-3649 (March 1965).

Allis, W. P., in Handbuch der Physik. ed. S. Flügge (Springer-Verlag, Berlin, 1956), Vol. XXL, p. 413.

Asundi, R. K., and J. D. Craggs, Proc. Phys. Soc. 83, 611 (1964).

Blatt, J. M., and V. F. Weisskopf, Theoretical Nuclear Physics (John Wiley and Sons, New York, 1963), p. 395.

Bortner, T. E., G. S. Hurst, and W. G. Stone, Rev. Sci. Instr. 28, 103 (1957).

Bortner, T. E., and G. S. Hurst, Health Phys. 1, 39 (1958).

Buchel'nikova, N. S., Soviet Phys.—JETP 35(8), 783 (1959).

Christophorou, L. G., R. N. Compton, G. S. Hurst, and P. W. Reinhardt, J. Chem. Phys. 43, 4273 (1965).

Christophorou, L. G., G. S. Hurst, and A. Hadjiantoniou, J. Chem. Phys. 44, 3506 (1966).

Christophorou, L. G., G. S. Hurst, and W. G. Hendrick, J. Chem. Phys. 45, 1081 (1966).

Christophorou, L. G., and R. N. Compton, Health Phys. 13, 1277 (1967).

Christophorou, L. G., R. N. Compton, and H. W. Dickson, J. Chem. Phys. (to be published).

Compton, R. N., L. G. Christophorou, G. S. Hurst, and P. W. Reinhardt, J. Chem. Phys. 45, 4634 (1966).

Compton, R. N., and L. G. Christophorou, Phys. Rev. 154, 110 (1967).

Fairstein, E., Rev. Sci. Instr. 29, 524 (1958).

Hamilton, N., and J. A. D. Stockdale, Aust. J. Phys. 19, 813 (1966).

Hasted, J. B., and S. Beg, Brit. J. Appl. Phys. 16, 74 (1965).

Hickam, W. M., and R. E. Fox, J. Chem. Phys. 25, 642 (1956).

Hurst, G. S., and T. E. Bortner, Rad. Res. Suppl. 1, 547 (1959).

Huxley, L. G., and R. W. Crompton, "The Motions of Slow Electrons in Gases," in Atomic and Molecular Processes. ed. D. R. Bates (Academic Press, New York, 1962), p. 336.

Jordan, W. H., and P. R. Bell, Rev. Sci. Instr. 18, 703 (1947).

Lowke, J. J., Aust. J. Phys. 16, 115 (1963).

Mahan, B. H., and C. E. Young, J. Chem. Phys. 44, 2192 (1966).

Pack, J. L., and A. V. Phelps, Phys. Rev. 121, 798 (1961).

Parks, J. E., and G. S. Hurst, "Studies of Electron Transport in Gases, Using Time-of-Flight Swarm Methods," Oak Ridge National Laboratory Report ORNL-TM-1287 (December 1965).

Rapp, D., and D. D. Briglia, J. Chem. Phys. 43, 1480 (1965).

Stockdale, J. A., and G. S. Hurst, J. Chem. Phys. 41, 225 (1964).

Stockdale, J. A. D., L. G. Christophorou, J. E. Turner, and V. E. Anderson, Phys. Letters 25A, 510 (1967).

INTERNAL DISTRIBUTION

1. Biology Library
2-4. Central Research Library
5. Reactor Division Library
6-7. ORNL Y-12 Technical Library Document Reference Section
8-57. Laboratory Records Department
58. Laboratory Records, ORNL R.C.
59. R. D. Birkhoff
60-84. L. G. Christophorou
85. R. N. Compton
86. F. J. Davis
87. C. E. Klots
88. W. H. Jordan
89. C. E. Larson
90. H. G. MacPherson
91. K. Z. Morgan
92. D. R. Nelson
93. P. W. Reinhardt
94. R. H. Ritchie
95. H. C. Schweinler
96. M. J. Skinner
97. W. S. Snyder
98. E. B. Wagner
99. A. M. Weinberg
100-109. G. S. Hurst (consultant)
110. D. Q. Brown (consultant)

EXTERNAL DISTRIBUTION

111. L. S. Anthony, Dept. of Physics, Roanoke College, Salem, Va.
112. J. B. Birks, Schuster Laboratory, University of Manchester, England.
113. T. E. Bortner, Dept. of Physics, University of Kentucky, Lexington, Ky. 40506.
114. J. C. Bowe, Radiological Physics Division, Argonne National Laboratory, Argonne, Ill. 60440.
115. H. H. Brongersma, F.O.M., Kruislaan 407, Amsterdam, Netherlands.
116. J.C.Y. Chen, Institute for Radiation Physics and Aerodynamics, University of California, LaJolla, California.
117. R. W. Crompton, Research School of Physical Sciences, The Australian National University, Ion Diffusion Unit, Box 4, G.P.O., Canberra, A.C.T. Australia.
118. D. C. Conway, Dept. of Chemistry, Texas A and M University, College Station, Texas 77843.
119. John V. Dugan, Lewis Laboratory, NASA, Cleveland, Ohio.
120. Florence Fayard, Laboratoire de Collisions Electroniques, Faculte des Sciences, Orsay (Essonne), France.
121. R. P. Ferrier, University of Cambridge, Cavendish Laboratory, Free School Lane, Cambridge, England.
122. G. R. Freeman, Dept. of Chemistry, University of Alberta, Edmonton, Canada.
123. D. C. Frost, University of British Columbia, Vancouver 8, Canada.

124. S. Hagström, Chalmers University of Technology, Dept. of Physics, Gibraltargatan 5B, Gothenburg S, Sweden.
125-134. W. G. Hendrick, Texas Nuclear Corporation, P. O. Box 9267, Allandale Station, Austin, Texas 78756.
135. W. P. Jesse, St. Procopius College, Physical Sciences Laboratory, Lisle, Illinois.
136. Joyce J. Kaufman, Quantum Chemistry Group, Research Institute for Advanced Studies, 1450 S. Rolling Rd., Baltimore, Md. 21227.
137. Lee J. Kieffer, Information Center, Joint Institute for Laboratory Astrophysics, University of Colorado, Boulder 80302.
138. T. King, The Physical Laboratories, The University, Manchester 13, England.
139. E. N. Lassettre, Mellon Institute, 4400 Fifth Avenue, Pittsburgh, Pennsylvania 15213.
140. Y. Leska, Fakulty of Science Komensky Univerzit Bratislava, Dept. of Organic Chemistry, Bratislava, Smeralova 2, Czechoslovakia.
141. R. J. Lovell, Dept. of Physics, University of Tennessee, Knoxville.
142. J. L. Magee, Radiation Laboratory, University of Notre Dame, Notre Dame, Indiana 46556.
143. E. W. McDaniel, Georgia Institute of Technology, School of Physics, Atlanta, Georgia 30332.
144. J. W. McGowan, Atomic Physics Laboratory, General Atomics, San Diego, California 92112.
145. T. F. Moran, Georgia Institute of Technology, School of Chemistry, Atlanta, Georgia 30332.
146. A. H. Nielsen, Dept. of Physics, University of Tennessee, Knoxville.
147. T. F. O'Malley, Defense Research Corporation, P. O. Box 3587, Santa Barbara, California 93105.
148. A. V. Phelps, Westinghouse Research Laboratories, Beulah Road, Pittsburgh, Pennsylvania 15235.
149. Foster F. Rieke, 203-C-149, Argonne National Laboratory, Argonne, Illinois 60440.
150. G. J. Schulz, Westinghouse Research Laboratories, Beulah Road, Pittsburgh, Pennsylvania 15235.
151. T. E. Sharp, Lockheed Missiles and Space Company, 3251 Hanover Street, Palo Alto, California 94304.
152. Bruce Steiner, National Bureau of Standards, Bldg. 221, Washington, D. C. 20234.
153. L. W. Swenson, Virginia Associate Research Center, 12070 Jefferson Avenue, Newport News, Virginia 23606.
154. H. S. Taylor, Dept. of Chemistry, University of Southern California, Los Angeles, California 90007
155. Ye-Yung Teng, University of Maryland, Dept. of Physics, College Park, Md. 20740.
156. Laboratory and University Division, AEC, ORO.
157-171. Division of Technical Information Extension
172. Oak Ridge Associated Universities, Fellowship Office.